

Monochromatization of Femtosecond X-Ray Free-Electron Laser Pulses by Means of Quasi-Forbidden Bragg Reflections from Periodic Multilayer Structures

V. A. Bushuev^a and L. Samoylova^b

^aMoscow State University, Moscow, 119991 Russia

^bEuropean XFEL GmbH, Hamburg 22607, Germany

e-mail: vabusuev@yandex.ru

Abstract—It is shown that the use of quasi-forbidden second-order reflections from a periodic multilayer structure $\text{Al}_2\text{O}_3/\text{B}_4\text{C}$ allows monochromatization of femtosecond X-ray free-electron laser pulses at level $\Delta E/E \approx 0.04\%$ with an efficiency of $\sim 60\%$. The intensity, shape, duration, and statistical characteristics of the reflected pulses are studied.

DOI: 10.3103/S1062873812020062

INTRODUCTION

The European X-Ray Laser (XFEL), emitting at a wavelength of ~ 0.1 nm, has undergone intense development in recent years [1]. Lasing in XFEL is based on the self-induced amplification of spontaneous emission (SASE [2]) of electron bunches of ~ 17.5 GeV in energy during their propagation through a system of superconducting undulators with a total length of ~ 120 m [1]. According to the calculations in [3–5], XFEL emission has the form of short pulses $\tau_0 \sim 100$ fs long with an extremely irregular multispikes structure, in which individual subimpulses (spikes) are $\tau_s \sim 0.1$ – 0.2 fs long and divided by time spans of ~ 0.3 – 0.4 fs. The cross dimension of a pulse at the undulator output is ≈ 70 μm , and the angular divergence is ≈ 1 μrad (in SASE channel 1) [4, 5].

Time resolution experiments and phase-contrast imaging depend substantially on the coherent properties of X-ray pulses. XFEL emission is almost totally spatially coherent and characterized by quite moderate temporal coherence [4, 5]. The length of spatial (lateral) coherence is comparable to the pulse cross dimension in the saturation mode, while the coherence time (longitudinal coherence) $\tau_c \approx \tau_s \approx 0.2$ fs $\ll \tau_0$, producing spectral pulse width $\Delta E/E \approx 0.1\%$ [4, 5].

Diffraction reflection from crystals and multilayer structures (MSes) is widely used for the monochromatization and collimation of X-radiation. The spectral XFEL pulse width exceeds the spectral width $\Delta E_B/E \leq 0.01\%$ of the Bragg reflection from perfect monocrystals by an order of magnitude and is much less than the width $\Delta E_B/E \sim 1$ – 5% of the diffraction reflection from typical periodic MSes. It was shown in [6] that reflected pulses are widened in time by 1–2 orders of magnitude during femtosecond pulse diffraction in crystals in the Bragg and Laue geometries, their shape

differs considerably from the temporal dependence of an incident pulse, and the peak intensity is equal to units and fractions of one percent.

It is of interest to analyze the possibilities of producing multilayer mirrors with the spectral interregion reflectance width $\Delta E_B/E \sim 0.05$ – 0.5% for practical purposes. In this work, we propose that the quasi-forbidden second-order Bragg reflection from an MS with a short period (~ 2 – 3 nm) based on light weakly absorbing elements (Al_2O_3 , B_4C , and BN) be used for these purposes. We have constructed a statistical theory of diffraction reflection and propagation of random transient femtosecond XFEL pulses. The MS parameters were analyzed for use as pulse splitters in the hard X-ray energy range. We should note that the use of glancing angles of incidence allows an increase in the radiation load of powerful XFEL pulses on an MS by about one order of magnitude, relative to the Bragg reflection from crystals.

PULSE PROPAGATION IN FREE SPACE

Let us first consider the propagation of an X-ray pulse from XFEL to arbitrary plane z [6–8]. Let us represent the pulse field in the source plane $z = 0$ (the output window of XFEL undulator) as

$$E(\vec{r}, 0, t) = A_s(\vec{r}, t) \exp(-i\omega_0 t), \quad (1)$$

where $\vec{r} = (x, y)$, ω_0 is the mean frequency, and A_s is a slowly varying and generally random and complex function. Let us represent amplitude (1) as an expansion in plane waves with frequencies $\omega = \omega_0 + \Omega$ and wave vectors $\vec{k} = (\vec{q}, k_z)$, satisfying the wave equation, where $k_z =$

$(k^2 - q^2)^{1/2}$, and $k = \omega/c$. Finally, for the pulse field in the plane z in the quasi-optic approximation,

$$E(\vec{r}, z, t) = A(\vec{r}, z, t) \exp(ik_0 z - i\omega_0 t), \quad (2)$$

where $k_0 = \omega_0/c = 2\pi/\lambda_0$, and the slowly varying amplitude

$$A(\vec{r}, z, t) = \int_{-\infty}^{\infty} \int_{-\infty}^{\infty} A_s(\vec{q}, \Omega) \exp[i\vec{q}\vec{r} - iq^2 z/2k - i\Omega(t - z/c)] d\vec{q} d\Omega. \quad (3)$$

Here $k = (\omega_0 + \Omega)/c$, the spectrum-angular amplitudes of the source radiation field

$$A_s(\vec{q}, \Omega) = (1/8\pi^3) \int_{-\infty}^{\infty} \int_{-\infty}^{\infty} A_s(\vec{r}, t) \exp(-i\vec{q}\vec{r} + i\Omega t) d\vec{r} dt. \quad (4)$$

In general, pulse (3) is spatially inhomogeneous and transient, since its correlation function depends on \vec{r} and t :

$$\Gamma_{tot}(\vec{r}, \vec{\rho}, z; t, \tau) = \langle A(\vec{r}, z, t) A^*(\vec{r} + \vec{\rho}, z, t + \tau) \rangle. \quad (5)$$

Let us represent the source field amplitude as the product of spatial and temporal functions $A_s(\vec{r}, t) = B_s(\vec{r})A(t)$. It then follows from Eqs. (3) and (4) that the pulse amplitude in plane z at $k \approx k_0$ is also equal to the product of two functions:

$$A(\vec{r}, z, t) = B(\vec{r}, z)A(t - z/c), \quad (6a)$$

$$B(\vec{r}, z) = \int_{-\infty}^{\infty} B_s(\vec{r}') G(\vec{r} - \vec{r}', z) d\vec{r}', \quad (6b)$$

where $G(\vec{\xi}, z) = (i\lambda_0 z)^{-1} \exp(i\pi \xi^2 / \lambda_0 z)$ is the propagator, $\vec{\xi} = (x - x', y - y')$.

Amplitude representation (6a) by the product of two functions results in a representation of total correlation function (5) in the form of the product of the spatial and temporal correlation function

$$\begin{aligned} \Gamma_{tot}(\vec{r}, \vec{\rho}, z; t, \tau) &= \Gamma_\rho(\vec{r}, \vec{\rho}, z) \Gamma(t, \tau), \quad \text{where} \\ \Gamma_\rho(\vec{r}, \vec{\rho}, z) &= \langle B(\vec{r}, z) B^*(\vec{r} + \vec{\rho}, z) \rangle, \\ \Gamma(t, \tau) &= \langle A(t) A^*(t + \tau) \rangle. \end{aligned} \quad (7)$$

As can be seen from Eq. (6a), the temporal pulse structure is invariable during propagation in free space. A Gaussian pulse in source plane $z = 0$ with amplitude $B_s(\vec{r}) = b_s(\vec{r}) \exp[-(r^2/2r_0^2)(1 - \alpha_0)]$ and the Gaussian spatial coherence function $\langle b_s(\vec{r}) b_s^*(\vec{r} + \vec{\rho}) \rangle = \exp(-\rho^2/\rho_0^2)$ also remains Gaussian at other distances z [7, 8]. Here, r_0 is the cross dimension of the pulse, ρ_0 is the spatial coherence length, and α_0 is the parameter describing the parabolic curvature of the wave front. The pulse cross dimension and the spatial coherence

length increase by M times with $r_1(z) = r_0 M$, $\rho_1(z) = \rho_0 M$, where

$$M(z) = [(1 + \alpha_0 D)^2 + D^2 + 2DW]^{1/2}, \quad (8)$$

and $D = \lambda_0 z / 2\pi r_0^2$, $W = \lambda_0 z / \pi \rho_0^2$ are the wave parameters. The amplitude quadratic phase parameter at distance z is $\alpha_1(z) = \alpha_0 + (1 + \alpha_0^2)D + 2W$. The pulse angular spectrum width $\langle |B(\vec{q}, z)|^2 \rangle = (2\pi \Delta q_0^2)^{-2} \exp(-q^2 / \Delta q_0^2)$ is defined by relationship [7]

$$\Delta q_0 = (1/r_0) [1 + \alpha_0^2 + 4(r_0/\rho_0)^2]^{1/2}. \quad (9)$$

The pulse angular divergence $\Delta\theta_0 = \Delta q_0/k_0 \leq 1 - 3 \mu\text{rad}$ for radiation with wavelength $\lambda_0 \sim 0.1 \text{ nm}$ at the typical XFEL parameters ($r_0 \approx 40 \mu\text{m}$, $\rho_0 \sim r_0$, and $\alpha_0 \leq 1$) [4], which is much less than the width of the diffraction reflection from an MS and even perfect crystals. Therefore, after reflecting from an MS, there is a further diffraction increase in the pulse cross dimension. At distance z_1 from an MS, $r_2(z + z_1) = r_1(z)M(z_1)$. If, e.g., $z \approx z_1 \approx 500 \text{ m}$, then $r_1 \approx 0.5 \text{ mm}$ and $r_2 \approx 1 \text{ mm}$.

Equations (6)–(9) are true at distances $z \ll z_c$, where $z_c \approx 2(E/\Delta E)/\pi\Delta\theta_0^2$ is the distance at which incomplete temporal coherence of the pulse begins to affect the spatial coherence and vice versa, as follows from Eq. (3). Condition $z \ll z_c$ is fulfilled in all cases of practical interest ($z_c \geq 1000 \text{ m}$) at pulse nonmonochromaticity $\Delta E/E \sim 10^{-3}$ and angular divergence $\Delta\theta_0 \sim 1 - 5 \mu\text{rad}$.

DIFFRACTION OF PULSES WITH RANDOM TIME STRUCTURE

Let us consider the effect of temporal incoherence and X-ray pulse nonstationarity on its diffraction reflection. Let us represent the random pulse amplitude $A(t)$ in Eq. (6a) in the form of Fourier integral over plane waves:

$$A(t) = \int_{-\infty}^{\infty} A(\Omega) \exp(-i\Omega t) d\Omega,$$

where spectral amplitude

$$A(\Omega) = (1/2\pi) \int_{-\infty}^{\infty} A(t) \exp(i\Omega t) dt.$$

Amplitude $A(t)$ is random; therefore, $A(\Omega)$ is also a random function. Each plane wave with amplitude $A(\Omega)$, incident on an MS, is reflected and propagates with the amplitude coefficients of reflection $R(\Omega)$ and propagation $T(\Omega)$; therefore, the slowly varying amplitudes of R - and T -pulses are defined by the integral

$$A_j(t) = \int_{-\infty}^{\infty} C_j(\Omega) A(\Omega) \exp[-i\varphi(\Omega, t)] d\Omega, \quad (10)$$

where $j = R, T$; $C_R = R, C_T = T$, $\varphi(\Omega, t) = \Omega(t - z/c)$, and z is the distance between the pulse and the MS.

The statistical properties of the reflected and propagating pulses are defined by the time correlation function

$$\Gamma_j(t, \tau) = \langle A_j(t)A_j^*(t + \tau) \rangle. \quad (11)$$

According to definition (11), pulse intensities $I_j(t) = \Gamma_j(t, 0)$. Let us substitute Eq. (10) into Eq. (11) and perform statistical averaging:

$$\begin{aligned} & \Gamma_j(t, \tau) \\ &= \int_{-\infty}^{\infty} \int_{-\infty}^{\infty} g(\Omega, \Omega') C_j(\Omega) C_j^*(\Omega') \Phi(\Omega, \Omega'; t, \tau) d\Omega d\Omega', \end{aligned} \quad (12)$$

where the spectral correlation function of incident pulse is defined as

$$g(\Omega, \Omega') = \langle A(\Omega)A^*(\Omega') \rangle, \quad (13)$$

and Φ is a regular function of frequency and time:

$$\Phi(\Omega, \Omega'; t, \tau) = \exp[-i\varphi(\Omega, t) + i\varphi(\Omega', t + \tau)]. \quad (14)$$

It follows from Eq. (13) that incident pulse spectrum $S(\Omega) = \langle |A(\Omega)|^2 \rangle = g(\Omega, \Omega)$. Eqs. (12)–(14) generally solve the problem of detecting intensities $I_j(t)$ and the temporal coherence functions $\gamma_j(t, \tau)$ of reflected and propagating pulses:

$$\gamma_j(t, \tau) = |\Gamma_j(t, \tau)| / [I_j(t)I_j(t + \tau)]^{1/2}. \quad (15)$$

The following simple model of transient XFEL pulses with random substructure can be suggested from an analysis of the data in [3–5]: $A(t) = F(t)a(t)$, where $F(t)$ describes the pulse envelope and is a regular time function; $a(t)$ is a random stationary process with mean $\langle a(t) \rangle = 0$, intensity $\langle a(t)a^*(t) \rangle = 1$, and correlation function $\gamma(\tau) = \langle a(t)a^*(t + \tau) \rangle$ independent of time. For such a random signal, $\langle a(\Omega)a^*(\Omega') \rangle = G(\Omega)\delta(\Omega - \Omega')$, where, according to the Wiener–Khinchine theorem, the spectral density (power spectrum) of the signal

$$G(\Omega) = (1/2\pi) \int_{-\infty}^{\infty} \gamma(\tau) \exp(-i\Omega\tau) d\tau. \quad (16)$$

The presence of a δ -shaped correlator allows conversion from the once-repeated integral in Eq. (13) to a simple integral and provides the following equation for the spectral correlation function:

$$g(\Omega, \Omega') = \int_{-\infty}^{\infty} F(\Omega - \Omega_1) F^*(\Omega' - \Omega_1) G(\Omega_1) d\Omega_1. \quad (17)$$

Let us assume below that incident pulse envelope $F(t)$ and the temporal coherence function of random stationary process $a(t)$ are Gaussian functions

$$F(t) = \exp(-t^2/2\tau_0^2), \quad \gamma(\tau) = \exp(-\tau^2/\tau_c^2), \quad (18)$$

where τ_0 is the pulse length and τ_c is the coherence time. The value of τ_0 is associated with total width Δt_0 of pulse intensity $I_m(t) = \langle |A(t)|^2 \rangle = F^2(t)$ at half height by relation $\tau_0 = \Delta t_0 / (2 \ln^{1/2} 2) = 0.6 \Delta t_0$. In addition to time τ_c in Eq. (18), the integral coherence time

$$\tau_M = \int_{-\infty}^{\infty} \gamma^2(\tau) d\tau, \quad (19)$$

introduced by Mandel in [9], is used.

If coherence function $\gamma(\tau)$ is Gaussian in form (18), then $\tau_M \approx 1.253 \tau_c$.

The diffraction intensity of a random pulse depends substantially on the relations between τ_0 and τ_c , or, which is the same, on the relationships between spectrum width $\Delta\Omega_0 = 1/\tau_0$ of incident pulse envelope $F(t)$, spectral width $\Delta\Omega_c = 2/\tau_c$ of temporal coherence function $\gamma(\tau)$, and characteristic width $\Delta\Omega_B$ of diffraction reflection curve $P_R(\Omega) = |R(\Omega)|^2$. Since $\tau_c \ll \tau_0$ for an XFEL pulse, such a pulse is quasi-stationary. In this case, it follows from Eqs. (17) and (18) that pulse spectrum $S(\Omega) \approx (\tau_0/2\pi^{1/2})G(\Omega)$, and its spectral width $\Delta\Omega \approx \Delta\Omega_c$ depends only on coherence time τ_c . A convenient equation for the relative width of the XFEL pulse spectrum can thus be derived: $(\Delta E/E)[\%] = 0.221 \times \lambda[\text{nm}]/\tau_M[\text{fs}]$.

It follows from Eqs. (12) and (17) that in the quasi-stationary case the temporal coherence function of reflected pulses is independent of time t :

$$\gamma_R(\tau) = \int_{-\infty}^{\infty} G(\Omega) |R(\Omega)|^2 \exp(i\Omega\tau) d\Omega. \quad (20)$$

A similar result is observed for the spatial coherence function of a MS-reflected cross-section random plane wave [8].

QUASI-FORBIDDEN BRAGG REFLECTION FROM AN MS FOR THE MONOCHROMATIZATION OF XFEL PULSES

The spectral width of a first-order reflection from a typical MS is about 1–5%, while the reflection from perfect monocrystals yields $\Delta E_B/E \sim 0.01\%$. It is interesting to discuss the possibility of producing MS with an intermediate reflection width, i.e., within the 0.05–0.5% range.

Coefficients $R(\Omega)$ and $T(\Omega)$ in Eq. (12) were calculated using both the Paratt recurrent formulae [10] and the analytical formulae of the dynamic diffraction theory in periodic structures of arbitrary thickness l [11]:

$$R = 2i\chi_h(\sin \varphi/Q), \quad T = (S/Q) \exp(-i\psi), \quad (21)$$

where $\varphi = k_0 l S / 4 \sin \theta_B$, $\psi = k_0 l \alpha / 4 \sin \theta_B$, $\alpha = 2 \sin 2\theta_B [\Delta\theta + (\Omega/\omega_0) \tan \theta_B]$, and

$$Q = S \cos \varphi - i\alpha_1 \sin \varphi, \quad S = (\alpha_1^2 - 4\chi_h \chi_{-h})^{1/2}.$$

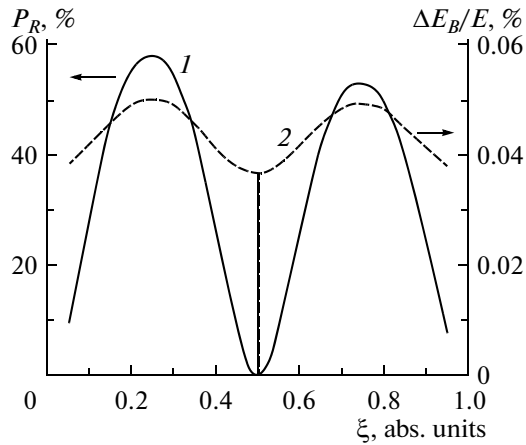


Fig. 1. Maximum second-order reflection intensity $P_R = |R|^2$ (curve 1) and spectral width of Bragg reflection $\Delta E_B/E$ (curve 2) as functions of relative layer thickness $\xi = d_1/d$. The parameters of the $\text{Al}_2\text{O}_3/\text{B}_4\text{C}$ MS are $d = 2.6$ nm, $\sigma = 0.2$ nm, $N = 1200$, $\lambda_0 = 0.1$ nm. Angle of incidence with respect to the MS surface $\theta = \theta_B = 2.21^\circ$.

Here $\alpha_1 = \alpha + 2\chi_0$, $\chi_{0, \pm h}$ are the Fourier components of the periodic MS polarizability function $\chi(z)$, $\Delta\theta = \theta - \theta_B$ is the offset of glancing angle θ relative to the Bragg angle θ_B , $l = Nd$, d is the MS period, and N is the number of periods. If the MS period consists of two layers with thicknesses d_1 and d_2 and polarizabilities χ_1 and χ_2 , then $\chi_0 = (\chi_1 d_1 + \chi_2 d_2)/d$,

$$\chi_h = (i/2\pi)(\chi_1 - \chi_2)f_{DW}F(m, \xi), \quad (22)$$

$$F(m, \xi) = m^{-1}[1 - \exp(i2\pi m\xi)],$$

where $F(m, \xi)$ is the MS structure factor, $\xi = d_1/d$, and $m = 1, 2, \dots$ is the reflection order. The effect of inter-layer roughness was considered in the Debye–Waller approximation [12]: $f_{DW} = \exp[-2(k_0 \sin\theta_B \sigma)^2]$. It is assumed that the rms roughness heights are σ for all layers. Layer polarizability $\chi = 2(n - 1)$ was calculated from the data in [13] for refractive indices $n = 1 - \delta + i\beta$.

Intensities of second-order Bragg reflection P_R and spectral widths $\Delta E_B/E$ when reflecting pulses with wavelength $\lambda_0 = 0.1$ nm from an $\text{Al}_2\text{O}_3/\text{B}_4\text{C}$ MS with period $d = 2.6$ nm and $\xi = 0.25$ at different numbers of periods N and rms heights of interlayer roughness σ . Bragg angle $\theta_B = 2.21^\circ$

	N	$\sigma = 0$	$\sigma = 0.1$ nm	$\sigma = 0.2$ nm
$P_R, \%$	800	63.3	56.0	35.5
	1200	83.8	78.5	58.4
	1600	91.8	88.7	74.1
$\Delta E_B/E, \%$	800	0.078	0.073	0.065
	1200	0.065	0.061	0.050
	1600	0.060	0.055	0.044

It follows from Eq. (21) that the relative spectral width of Bragg reflection $\Delta E_B/E \approx |\chi_h|/\sin^2\theta_B$ at a sufficiently large number of periods $N \geq N_{ex}$, where $N_{ex} \approx 2\Lambda/d$, $\Lambda = \lambda_0 \sin\theta_B/\pi|\chi_h|$ is the extinction depth. To reduce width $\Delta E_B/E$, we use an MS with short period d , which increases Bragg angle θ_B , and weakly absorbing substances with low contrast $\chi_1 - \chi_2$. In this case, however, the number of periods must be increased to $N \sim 200 - 800$ [14, 15].

Structural factor $F(m, \xi)$ (22) for a first-order reflection is maximal at $\xi = 0.5$ and equal to 2; it follows that $N_{ex} \approx 2\sin^2\theta_B/((\delta_1 - \delta_2)f_{DW})$. If we consider the most promising MS $\text{Al}_2\text{O}_3/\text{B}_4\text{C}$ [14, 15] with $d = 2.5$ nm and $\sigma = 0.3$ nm, then Bragg angle $\theta_B = 1.16^\circ$, $(\delta_1 - \delta_2) = 2.08 \times 10^{-6}$, and number of periods $N_{ex} \approx 510$ at $\lambda_0 = 0.1$ nm. At such N , Bragg reflection curve maximum $P_R(\Omega = 0) = 88.3\%$ and spectral width $\Delta E_B/E = 0.34\%$ (here and below, the spectral width is defined as the total width at a half of height). Raising the number of periods does not increase the intensity of reflection or reduce the spectral width. At best, we can attain $\Delta E_B/E \sim 0.2 - 0.4\%$ at $N \sim 10^3$ and $\sigma \leq 0.3$ nm in the case of a first-order reflection from an $\text{Al}_2\text{O}_3/\text{B}_4\text{C}$ MS with period of $d \sim 1.5 - 3$ nm; this sets high requirements on the degree of MS perfection.

Let us now consider a second-order reflection. Structural factor $F(m, \xi)$ is zero (a forbidden reflection) at $m = 2$ and previous value $\xi = 0.5$. To reduce width $\Delta E_B/E$ further, we propose using MSes with quasi-forbidden reflections, i.e., structures with $\xi \neq 0.5$, for which $F(2, \xi) \neq 0$. Figure 1 and Table 1 show that a sufficiently high reflection intensity ($P_R \approx 60\%$) with the very narrow spectral width $\Delta E_B/E \approx 0.04\%$ can be implemented for a second-order reflection at $\xi \approx 0.25$ and 0.75 . Table 1 shows that the intensity of the Bragg maximum increases with the number of periods while the reflection spectral width decreases, as would be expected. An increase in the height of roughness naturally results in a reduction in the intensity of reflection. The narrowing of the spectral width (at fixed N) with increasing height of roughness σ is a rather interesting effect. The narrowing of reflection curve $P_R(\Omega)$ is due to the roughness suppressing the edges of the function more strongly.

In Fig. 2., the spectrum of an incident XFEL pulse, normalized to unity $G(\Omega)$ and with coherence time $\tau_M = 0.22$ fs, is compared to the spectral intensity of a second-order Bragg reflection $P_R(\Omega)$ from an $\text{Al}_2\text{O}_3/\text{B}_4\text{C}$ MS. It can be seen that reflection spectrum width $\Delta E_B/E$ is almost half the spectral width of the incident pulse.

As in the case of perfect crystals [6], a reflection from an MS with a narrow reflection coefficient results in the distortion of temporal dependence $I_R(t)$ of the reflected pulse intensity, relative to the profile $I_{in}(t)$ of an incident pulse (Fig. 3), and in a change in the shape and width of the temporal coherence function (Fig. 4). Intensity $I_R(t) = \Gamma_R(t, 0)$ was calculated by Eq. (12),

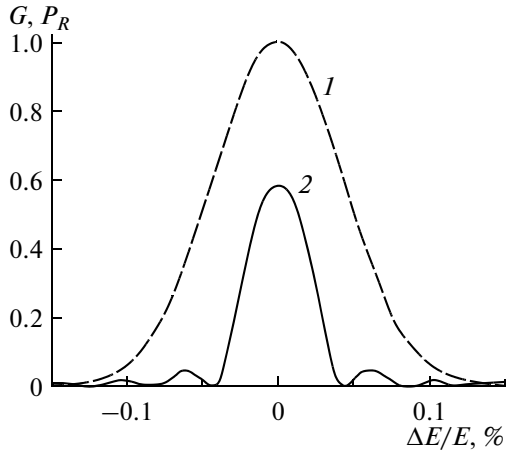


Fig. 2. Spectral intensity $G(\Omega)$ of a XFEL pulse with width $\Delta E/E = 0.1\%$ (curve 1) and curve of reflection $P_R(\Omega)$ (curve 2) from an $\text{Al}_2\text{O}_3/\text{B}_4\text{C}$ MS with $\xi = 0.25$. Pulse length $\tau_0 = 100$ fs; coherence time $\tau_M = 0.22$ fs. Other parameters are the same as in Fig. 1.

and the temporal coherence function of a reflected pulse $\gamma_R(\tau)$, according to Eq. (20).

The pulse amplitudes in Fig. 3 were specified by the equation $A_1 \exp(-t^2/\tau_s^2)$ and $A_2 \exp[-(t - t_{12})^2/\tau_s^2]$ (where $\tau_s = 0.125$ fs and $t_{12} = 0.4$ fs) and considered independent, i.e. incoherent in time. The relative width of the pulse spectrum is 0.1% at pulse length τ_s , which agrees with the calculations of the random time structure and the XFEL pulse spectrum width in [4, 5]. As can be seen from Fig. 3, the two short incoherent pulses that in this case represent the model of random spikes in XFEL pulses overlap strongly and widen after reflection [6, 16]. The reflected pulse intensity falls by about a factor of almost 11 after the first reflection in a twofold monochromator (curve 2). The second reflection results in a lower reduction in intensity (by a factor of 2.7), which is explained by the narrowing of pulse spectrum $I_{R1}(t)$. The lengths of the reflected pulses considerably exceed spike lengths τ_s , and the time span between them.

Reflection from an MS also results in a widening of the temporal coherence function by a factor of almost 2.5 and in symmetrical damped oscillations at the tails of the function $\gamma_R(\tau)$ (see Fig. 4). A similar result was earlier obtained for the spatial coherence function during reflection of spatially partly coherent and temporally stationary X-ray beams from MS [8].

CONCLUSIONS

A statistical diffraction theory of X-ray pulses with random time structure has been developed. We have shown that a quasi-forbidden reflection of femtosecond XFEL pulses from MS results in certain mono-

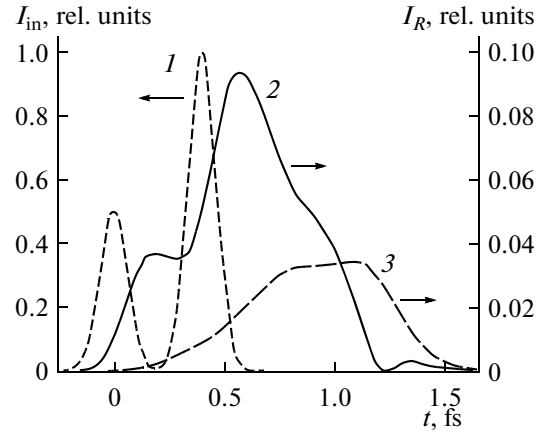


Fig. 3. Effect of Bragg reflections of an MS in a twofold monochromator on the intensity and shape of reflected pulse $I_R(t)$ after the first (curve 2) and second (curve 3) reflections. Incident pulse $I_{in}(t)$ (curve 1) consists of two incoherent pulses with equal lengths of 0.15 fs and amplitudes $A_1 = 0.7$ and $A_2 = 1$. The time span between the pulses is equal to 0.4 fs. Parameter $\xi = 0.25$; all other parameters are the same as in Fig. 1.

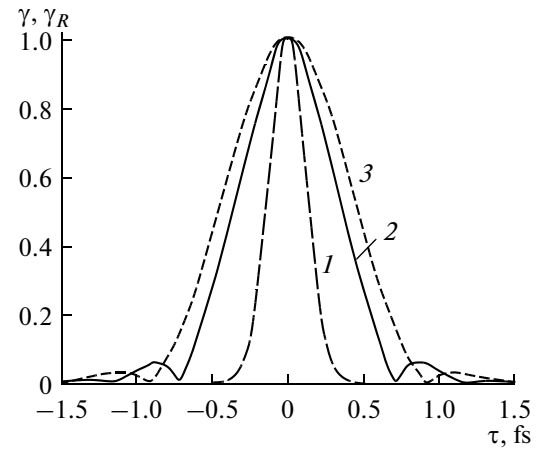


Fig. 4. Temporal coherence function of an incident pulse $\gamma(\tau)$ (curve 1) and a reflected pulse $\gamma_R(\tau)$ after the first (2) and second (3) reflections. The coherence times $\tau_M = 0.22$ fs, $\tau_{MR1} = 0.54$ fs, and $\tau_{MR2} = 0.69$ fs. All other parameters are the same as in Figs. 1 and 2.

chromatization, or, in other words, in a widening of the temporal coherence function. To a certain degree, interlayer roughness with reasonable limits on height even facilitates the production of MSes with a Bragg reflection width in the range between conventional MSes and perfect monocrystals.

ACKNOWLEDGMENTS

V. A. Bushuev is grateful to the Russian Foundation for Basic Research (grant no. 10-02-00768) and the FRG Ministry for Education and Research (project

no. 05K10CHG) for their financial support. The authors are grateful to M. Yurkov for the 3D FAST calculation results on SASE 1 XFEL pulses, and to M. Yurkov, H. Sinn, and Th. Tschentscher for their useful discussions.

REFERENCES

1. *XFEL, Technical Design Report, DESY 2006–097*, Altarelli, M., et al., Eds., Hamburg, 2006. http://xfel.desy.de/tdr/index_eng.html
2. Saldin, E.L., Schneidmiller, E.A., and Yurkov, M.V., *The Physics of Free Electron Lasers*, Berlin: Springer, 1999.
3. Saldin, E., Schneidmiller, E., and Yurkov, M., *Nucl. Instrum. Methods. A*, 1999, vol. 429, nos. 1–3, p. 233.
4. Geloni, G., Saldin, E., Samoylova, L., et al., *New J. Phys.*, 2010, vol. 12, no. 3, p. 035021.
5. Saldin, E.L., Schneidmiller, E.A., and Yurkov, M.V., *New J. Phys.*, 2010, vol. 12, no. 3, p. 035010.
6. Bushuev, V.A., *J. Synchrotron Rad.*, 2008, vol. 15, no. 5, p. 495.
7. Bushuev, V.A., *Bull. Russ. Acad. Sci. Phys.*, 2009, vol. 73, no. 1, p. 52.
8. Bushuev, V.A., *Bull. Russ. Acad. Sci. Phys.*, 2010, vol. 74, no. 1, p. 41.
9. Mandel, L., *Proc. Phys. Soc.*, 1959, vol. 74, no. 3, p. 223.
10. Parratt, L.G., *Phys. Rev.*, 1954, vol. 95, no. 2, p. 359.
11. Authier, A., *Dynamical Theory of X-Ray Diffraction*, New York: Oxford Univ. Press, 2001.
12. Nevot, L. and Croce, P., *Rev. Phys. Appl.*, 1980, vol. 15, no. 3, p. 761.
13. <http://www.esrf.eu/UsersAndScience/Experiments/TBS/SciSoft>
14. Martynov, V.V., Platonov, Yu., Kazimirov, A., and Bilderbrack, D.H., *AIP Conf. Proc.*, 2004, vol. 705, no. 5, p. 697.
15. Kazimirov, A., Smilgies, D.-M., Shen, Q., et al., *J. Synchrotron Rad.*, 2006, vol. 13, no. 2, p. 204.
16. Shastri, S.D., Zambianchi, P., and Mills, D.M., *J. Synchrotron Rad.*, 2001, vol. 8, no. 11, p. 1131.